

Self-passivation of austenitic steel 316 L and its welded joints in sulphuric acid

The spontaneous (self) – passivation and/or electrochemical passivation processes on austenitic steel 316 L and its welded joints were studied in deaerated sulphuric acid (1.7 M) at room temperature. Electrodes were prepared from materials taken from the central zone of the weld (zone 1), the so called overheated zone - OHZ (or temperature affected zone) (zone 2) and basic material - BM (zone 3). It has been concluded that the austenitic steel 316 L and its welded joints indicate the existence of self-passivation processes (passive corrosion) in deaerated sulphuric acid with formation of oxide-passive films (mainly Fe-Cr oxides) at the metal surface with thickness of 1-1.5 nm. As it was shown the corrosion behaviour of the welded material mainly depends on the chemical stability and the thickness of the passive film formed at the surfaces of the various zones. It can be also, concluded that the corrosion process is mainly located on the border of the fusion line OHZ-BM.

Key words: self-passivation, austenitic steel 316 L, welding, corrosion properties

1. INTRODUCTION

The phenomenon of passivity is a remarkable one, remarkable because of the extremely thin film required to procure passivity. The typical passivating oxide film on many metals is only some 1-10 nm in thickness, and is produced by oxidation of the surface to a depth measured in monolayers of atoms. Without the passivating oxide film many metallic structures would corrode at a very fast rate, phenomenological evidence for this being provided by the very fast rates at which localised corrosion (such as pitting corrosion or stress-corrosion cracking) can propagate when passivity is disrupted and regeneration of the passivating oxide film cannot take place. Despite the great deal of information and knowledge that has thereby been generated, there are many questions that remain to be answered before a full understanding of the subject is achieved.

Stainless steels, which contain highly passive components (such as chromium), owe their corrosion resistance to the surface enrichment of the passivating component [1]. Thus stainless steels resist corrosion in many acidic systems (where iron or carbon steel would be poorly passive or not passive at all) by a passivating oxide film containing Cr predominantly as Cr(III). Surface analytical techniques such as Auger electron and X-ray photoelectron spectroscopies reveal substantial enrichment of chromium in the passivating oxide film on these alloys [2, 3].

The spontaneous (self) - passivation processes of austenitic (Cr-Ni) steels in the usual corrosion envi-

ronments (atmosphere, natural waters, soils, electrolytes etc.) with formation of a thin (1-3 nm) oxide-films of Fe-Cr-Ni-oxides (bad ionic and electronic conductors), is a main reason for a high corrosion stability of this material [4-9].

The aim of this work is to give some more evidences for the electrochemical and corrosion behaviour of the welded joints of metallic equipment.

2. EXPERIMENTAL

The working electrodes were prepared from austenitic steel 316 L (7 x 7 x 5 mm; mounted in Teflon holder) taken from the central zone of the weld (zone 1; $A \approx 0.53 \text{ cm}^2$), the so called overheated zone or temperature affected zone (OHZ); $A \approx 0.55 \text{ cm}^2$ (zone 2) and basic material, zone 3 (BM); $A \approx 0.525 \text{ cm}^2$, Figure 1.

The electrode surfaces were mechanically polished with emery paper 600 and diamond spray (1 and 0.3 μm). Finally, the electrodes were carefully rinsed with distilled water and ultrasonically cleaned in ethanol.

A Pt foil ($\sim 10 \text{ cm}^2$) and Hg/Hg₂SO₄/H₂SO₄ electrode were used as the counter and reference electrode, respectively. All the measured potentials are referred to the standard hydrogen electrode (she).

A classical three-compartment cylindrical electrolytic cell equipped with Luggin capillary and an inlet and outlet for bubbling inert gas was used. The solution in the cell was initially deaerated by flowing nitrogen gas through a fritted bubbler for a least 30 min prior to the run.

Aqueous solution of 15 w% (1.7 M) sulphuric acid was prepared from concentrated H₂SO₄ (96-98 % H₂SO₄ p.a. - Merck) with redistilled water ($\chi < 2 \cdot 10^{-7} \text{ Scm}^{-1}$).

Address authors: Faculty of Technology and Metallurgy, "St. Cyril and Methodius University", Skopje, R. Macedonia

The potentiostatic and potentiodynamic measurements were performed after electrochemical pretreatment of the electrode at low cathodic potential (-0.25 V/she) for 10 minutes and the open circuit potential (OCP) decay has been followed for 200 minutes. The experiments were carried out at room temperature.

The EIS (Electrochemical Impedance Spectroscopy) measurements were carried out in the frequency range from 100 kHz to 10 mHz (with a.c. signal of 5 mV) at several potentials: -0.15 ; 0.3 ; 0.7 and 0.9 V/she. It should be mentioned that the working electrode was treated for approx. 10 minutes at these specified potentials (-0.15 V; 0.3 ; 0.7 V and 0.9 V/she) before every run of impedance measurement.

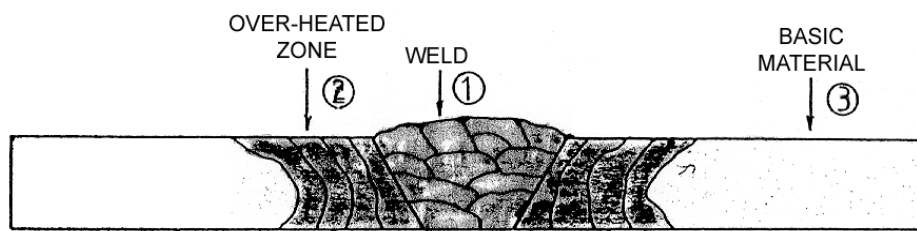


Figure 1 - Schematic representation of welded part (steel 316 L): weld - zone 1; overheated zone – zone 2 and basic material – zone 3.

3. RESULTS AND DISCUSSION

Open circuit and potentiodynamic measurements:

As can be seen from Figure 2 the austenitic steel 316 L and its welded joints clearly show self-passivation properties. These processes, followed with relatively fast anodization of the open circuit potential (OCP) indicate the formation of oxide (passive) layer at the electrode surface proved with Electrochemical Impedance Spectroscopy (EIS). Mainly, three potential steps (regions) can be distinguished on these curves. Comparing these characteristic potentials with those marked on the

voltammograms, Figure 3, it can be concluded:

- The first step ($-0.02 \div 0.03$ V/she) appears in the active region of electrochemical dissolution ($\text{Fe} - 2\text{e}^- = \text{Fe}^{2+}$), where the anodic current sharply increases linearly with scanning potential (region A-B).
- The second step ($0.07 \div 0.11$ V/she) belongs to the end of the electrochemical dissolution process (primary passivation potential - point B).
- The third step ($0.12 \div 0.27$ V/she), corresponds to the beginning of the "real" passivation process (point C).

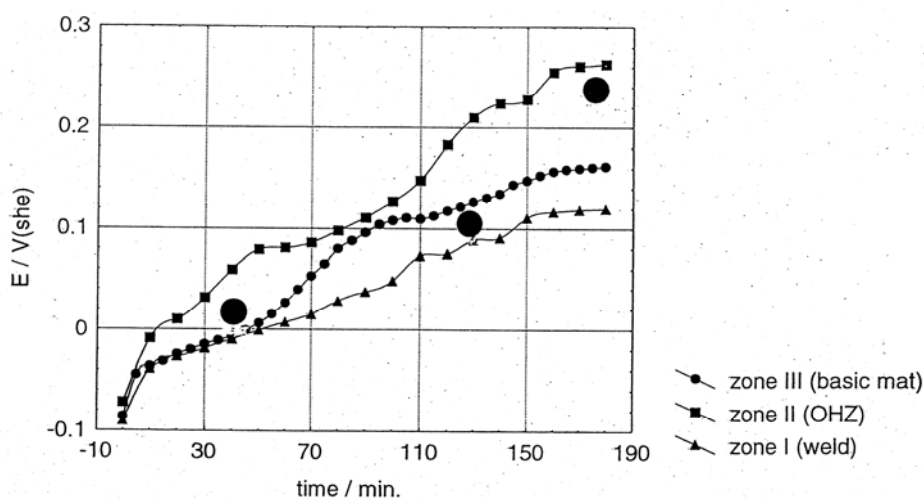


Figure 2 - OCP / time - dependences for spontaneous passivation of steel 316 L in deaerated 1.7 M H_2SO_4 (after cathodic pretreatment at -0.25 V/she for 10 min.) at room temperature.

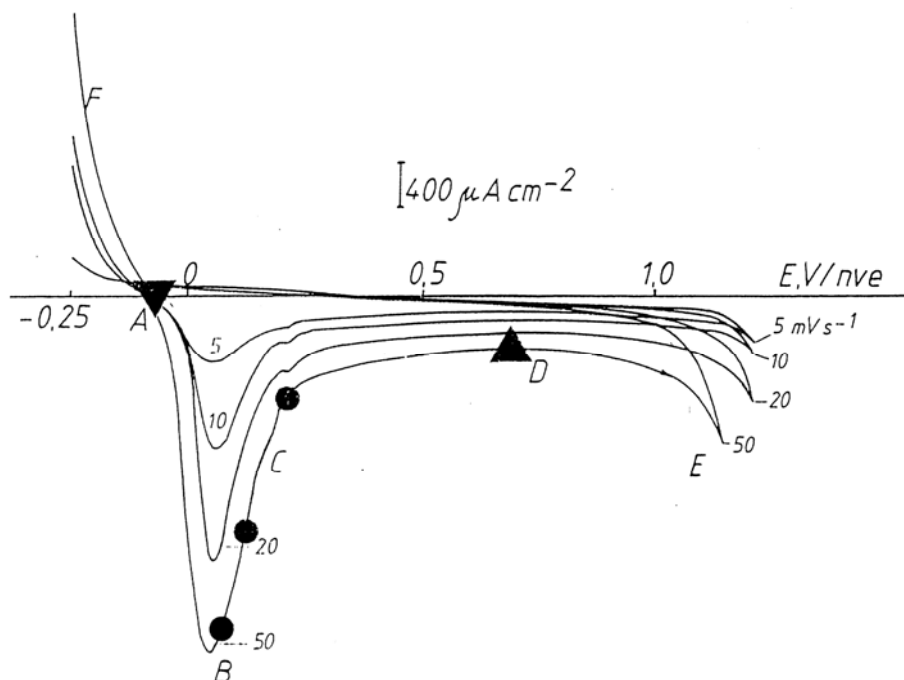


Figure 3 - Cyclic voltammograms for electrochemical passivation of austenitic steel 316 L, basic material – zone 3 in 1.7 M H_2SO_4 , at room temperature.

The above-mentioned considerations for self-passivation processes of austenitic steel 316 L were additionally confirmed with experiments presented in Figure 4.

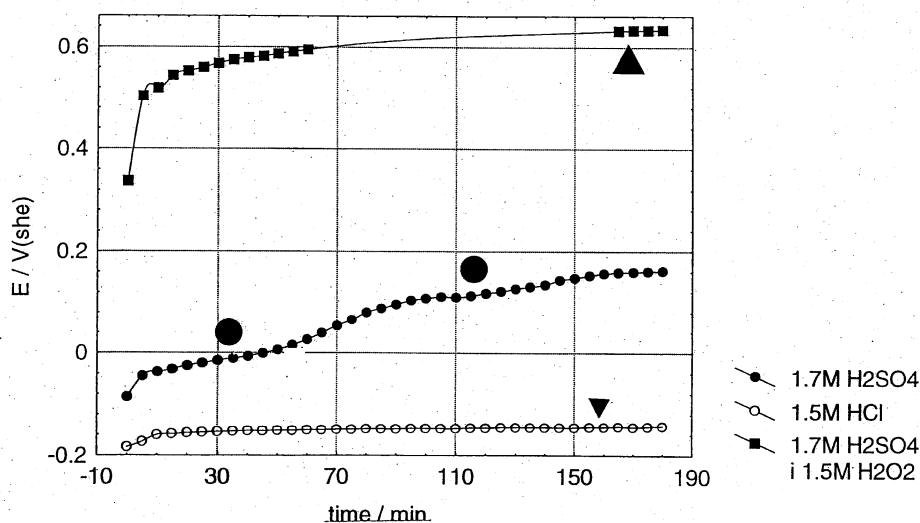


Figure 4 - OCP / time - dependences for spontaneous passivation of steel 316 L in several deaerated acidic solutions, basic material - zone 3 (after cathodic pretreatment at - 0.25 V/she for 10 min.), room temperature.

Evidently, in a strong acidic media (1.5 M HCl) and the presence of significant concentration of de-passivation anions (Cl^-), the value of OCP (from - 0.19 to - 0.15 V/she) is almost constant with time, indicating that the active corrosion take place at the steel surface (point A, Figure 3).

On the other hand, in the presence of a strong oxidant (1.5 M H_2O_2) the process of self-passivation of austenitic steel 316 L is extremely fast. It is evident that the value of the final OCP (~ 0.6 V) was achieved in a relatively short period and according with Figure 3 is located in the middle of the passive region (point D).

Electrochemical Impedance Spectroscopy (EIS)

In order to characterize the metal/H₂SO₄ and/or metal/oxide/ H₂SO₄ interfaces of the austenitic steel 316 L and its welded joints, the EIS - measurements were carried out at several potentials: -0.15; 0.3; 0.7 and 0.9 V/she (see Fig. 3) and frequency range from 100 kHz to 10 mHz (with a.c. signal of 5 mV). The obtained experimental results were fitted with Boukamp program [10] using the simple equivalent electric circuit (EEC) – $R(QR)$, Fig. 5 (where R_{el} is ionic resistance of electrolyte; CPE is constant phase element characterize with Q and n and R_{ct} or R_{ox} are

charge transfer resistances in the absence or the presence of oxide at the metal surfaces).

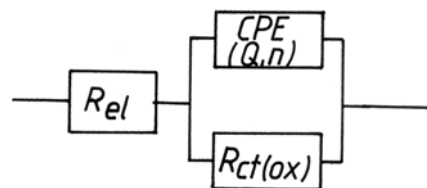


Figure 5 - Equivalent electric circuit for impedance characterization of metal/solution and metal/oxide/solution-interface.

Table 1 - Best fitting parameters for systems: metal/H₂SO₄ and/or metal/oxide/ H₂SO₄ interfaces using a simple $R(QR)$ -EEC

Zone	$E/V(\text{she})$	$R_{el}/\Omega\text{cm}^2$	$Q/\Omega^{-1}\text{s}^n$	n	$C/\mu\text{Fcm}^{-2}$	$R_{ct}^*(R_{ox})/\text{k}\Omega\text{cm}^2$	L_{ox}/nm
1 (weld)	-0.15	2.00	$1.01 \cdot 10^{-4}$	0.79	16.50	0.52*	-
	0.3	2.50	$1.18 \cdot 10^{-4}$	0.76	12.80	1.30	1.04
	0.7	2.50	$8.63 \cdot 10^{-5}$	0.76	8.50	1.43	1.56
2 (OHZ)	-0.15	1.50	$5.76 \cdot 10^{-5}$	0.85	18.80	0.58*	-
	0.3	1.50	$1.054 \cdot 10^{-4}$	0.77	12.50	0.73	1.06
	0.7	1.50	$6.12 \cdot 10^{-5}$	0.81	11.50	0.90	1.15
	0.9	1.50	$5.08 \cdot 10^{-5}$	0.81	9.14	1.11	1.45
3 (BM)	-0.15	1.20	$5.54 \cdot 10^{-5}$	0.85	18.70	0.70*	-
	0.3	1.20	$5.34 \cdot 10^{-5}$	0.84	15.60	1.11	0.85
	0.7	1.20	$4.13 \cdot 10^{-5}$	0.84	11.50	1.22	1.15
	0.9	1.20	$3.10 \cdot 10^{-5}$	0.86	10.90	1.51	1.22

These data indicate:

- The obtained values of Q (constant phase element – CPE; $Z = (1/Q(j\omega)^n)$ or $C = Q^{1/n}$), Table 1, are strongly influenced by the electrode potential or the thickness of the electrochemically formed passive films. These values are in a good agreement with usual literature data (stainless steel 316 L/acidic solution). The thicknesses of the passive films were calculated using data from Table 1 and equation:

$$L_{ox} = \varepsilon_{ox} / 1.13 C_{ox} [nm],$$

where C is given in μFcm^{-2} , for $\varepsilon=15$ [11].

- The double layer capacities (dlc) of the austenitic steel 316L/solution interface at -0.15 V/she is mainly determined by the adsorbed layer of the solvent (H₂O) molecules ($d_{\text{H}_2\text{O}} \approx 0.4 \text{ nm}$) [12] and ranged between 16.5 and 18.80 μFcm^{-2} .

- The values of the charge transfer resistance (R_{ct}) (or oxide resistance (R_{ox})), Figs.6-8, of the electrochemically formed passive films, Table 1, depend on the electrode potential of passivation and from the zone of austenitic steel.

- Using these data the corrosion currents of the presented systems can be calculated by the equation: $j_{\text{corr}} = (RT/zF) \cdot (1/R_{ct})$ (given in Table 2). The rates of corrosion, Table 2, ranged between 0.29 and 0.1 mmy^{-1} and regularly depend on the electrode potential (with and/or without passive film at the metal surface).

The protection properties of the passive films formed by self and/or electrochemical passivation of the electrode surfaces ranged between 50 and 65 %, depending, also of the type of the welded material zone (weld, OHZ and BM).

- As can be seen from the presented values of the j_{corr} (v_{corr}), Table 2, for a constant electrode potential, the OHZ is much more affected by the corrosion process comparing with the other two zones of the welded material.

The calculated values of the passive-oxide films resistivity ranged between $7.8 \cdot 10^9$ and $1.1 \cdot 10^{10} \Omega\text{cm}$ indicating formation of a compact and homogeneous protective film at the steel surface ($\rho_{ox} = R_{ox} \cdot A / L_{ox}; \Omega\text{cm}$).

Table 2 - Electrochemical parameters for the system: stainless steel 316 L and its welded joints in 1.7 M H₂SO₄ at room temperature.

Zone	E/V(she)	$R_{ct}^*(R_{ox})/k\Omega\text{cm}^2$	L_{pf}/nm	$j_{corr}/\mu\text{Acm}^{-2}$	v_{corr}/mmy^{-1}
1 (weld)	-0.15	0.52*	-	25.00	0.290
	0.3	1.30	1.04	10.00	0.116
	0.7	1.43	1.56	8.94	0.104
2 (OHZ)	-0.15	0.58*	-	22.40	0.260
	0.3	0.73	1.06	17.80	0.210
	0.7	0.90	1.15	14.40	0.170
	0.9	1.11	1.45	11.70	0.136
3 (BM)	-0.15	0.70*	-	18.60	0.220
	0.3	1.11	0.85	11.80	0.137
	0.7	1.22	1.15	10.52	0.122
	0.9	1.51	1.22	8.50	0.099

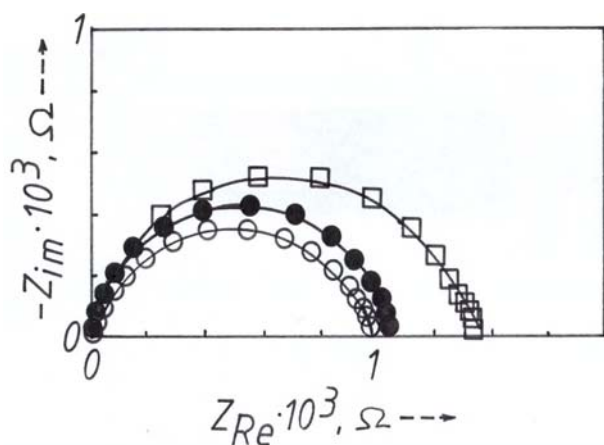


Figure 6 - Experimental (\circ ; \bullet ; \square) and theoretical (—) Nyquist plots for austenitic steel 316L (weld - \circ -; OHZ - \bullet - and BM - \square -) in deaerated 15 % (1.7 M) H₂SO₄ at -0.15 V/she and room temperature using R(QR)-EEC.

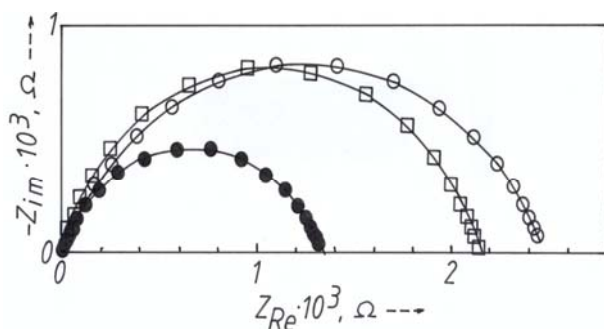


Figure 7 - Experimental (\circ ; \bullet ; \square) and theoretical (—) Nyquist plots for austenitic steel 316L (weld - \circ -; OHZ - \bullet - and BM - \square -) in deaerated 15 % (1.7 M) H₂SO₄ at 0.3 V/she and room temperature using R(QR)-EEC.

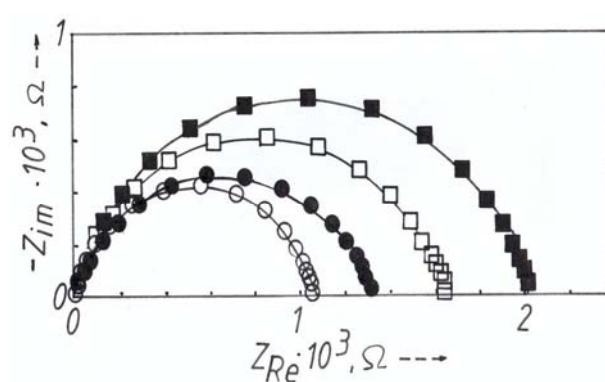


Figure 8 - Experimental (\circ ; \bullet ; \square ; \blacksquare) and theoretical (—) Nyquist plots for austenitic steel 316L (OHZ) in deaerated 15 % (1.7 M) H₂SO₄ at -0.15 (- \circ -); 0.3 (- \bullet -); 0.7 (- \square -) and 0.9 (- \blacksquare -) V/she and room temperature using R(QR)-EEC.

4. CONCLUSIONS

Electrochemical and impedance study (EIS) of the austenitic steel 316 L and its welded joints in deaerated sulphuric acid at room temperature unambiguously show the existence of self-passivation processes with formation of passive films (mainly Fe-Cr oxides) with thickness of 1-1.5 nm.

As it was shown the corrosion behaviour of the welded material mainly depends on the chemical stability and the thickness of the passive film formed at the various zones surfaces.

It can be also, concluded that the corrosion process is mainly located on the border of the fusion line OHZ-BM.

REFERENCES

- [1] W. H. J. Vernon, F. Wormwell and T. J. Nurse, **J. Iron Steel Inst.**, 150, 81, 1944
- [2] M. Froment (Ed.), **Passivity of Metals and Semiconductors**, Elsevier, Amsterdam, 1983.
- [3] B. R. MacDougall, R. S. Alwitt and T. A. Ramana-
rayanan (Eds), **Oxide Film on Metals and Alloys**,
Proceedings, 92-22, The Electrochemical Society,
Pennington, New Jersey, 1992.
- [4] U. Konig, M. Beier and J.W. Schultze, **ISIJ Inter-
national**, 31, 142-148, 1991.
- [5] R. Kirchheim, B. Heine, H. Fishmeister, S. Ho-
fmann, H. Knote and U. Stolz, **Corros. Sci.**, 29,
899-917, 1989.
- [6] S. Haupt, H.H. Strehblow, **Corros. Sci.**, 37, 43-54,
1995.
- [7] C.O.A.Olsson and D. Landolt, **Electrochim. Acta**,
48, 9, 1093-1104, 2003
- [8] C.Garsia, M.P.de Tiedra, Y.Blanco, O.Martin and
F.Martin, **Corros. Sci.**, 50, 8, 2390-2397, 2008
- [9] B.T.Lu, Z.K.Chen, J.L.Luo, B.M.Patchett and
Z.H.Xu, **Electrochim. Acta**, 50, 6, 1391-1403,
2005.
- [10] B.A. Boukamp, Equivalent circuit, **Solid State
Ionic**, 20, 31-38, 1986.
- [11] M.M.Lohrengel, K.Schubert and J.W.Schultze,
Werkst. Korros., 32, 13, 1981.
- [12] D.Chamovska, M.Cvetkovska, T.Grchev, **Bull.
Chem. Technol. Macedonia**, 18, 187-197, 1999.